

Molecular analysis of recombinase-mediated cassette exchange reactions catalyzed by integrase of coliphage HK022

Natalia Malchin, Tatiana Molotsky, Ezra Yagil, Alexander B. Kotlyar, Mikhail Kolot*

Department of Biochemistry, Tel-Aviv University, Ramat-Aviv, Tel-Aviv 69978, Israel

Received 31 July 2008; accepted 5 September 2008

Available online 24 September 2008

Abstract

The integrase (Int) protein of coliphage HK022 can catalyze in *Escherichia coli* as well as in in vitro integrative and excisive recombinase-mediated cassette exchange reactions between plasmids as substrates. Atomic force microscopy images have revealed that in the protein–DNA complexes that are formed, the plasmid substrates are connected via one and not two pairs of attachment sites. This observation, together with the elucidation of intermediate co-integrates between the two circular plasmids, suggest that a sequential mechanism of the RMCE reaction is possible.

© 2008 Elsevier Masson SAS. All rights reserved.

Keywords: Site-specific recombination; Integrase; Bacteriophage HK022; Recombinase-mediated cassette exchange; Atomic force microscopy

1. Introduction

Site-specific recombination systems of lower organisms have become important tools for site-specific gene manipulations in eukaryotic organisms. These include insertions, deletions and activation of genes [3,6,19]. A recent important approach is recombinase-mediated cassette exchange (RMCE) technology in which a desired gene or any other chromosomal DNA fragment can replace a predefined chromosomal fragment. This is accomplished when the chromosomal fragment is flanked by two incompatible site-specific recombination sites and the replacing DNA is likewise flanked by the same recombining sites. The relevant site-specific recombinase can catalyze an exchange between the chromosomal fragment and the replacing DNA. The two incompatible pairs of sites can be substrates of the same recombinase [18] or substrates of two different recombinases [16,23]. In case of a single recombinase, one pair of compatible sites should be mutated in order to be incompatible with the wild-type sites. The use of mutated sites is less efficient and may still cause some undesired compatibility between the two flanking recombination sites [5,15].

Integrase (Int), the site-specific recombinase of coliphage HK022, catalyzes the reaction of the phage's lysogenic pathway in a mechanism that is very similar, if not identical, to that of well known coliphage λ . In both phages, Int catalyzes the integration and excision reactions by pairs of non-identical recombination sites (*att*) that differ in size and sequence, except for a 7-base pair (bp) core sequence that is the site of recombination and is identical in all four *att* sites. *attP* (246 bp) + *attB* (21 bp) are the sites of phage integration and their recombination products *attL* (101 bp) + *attR* (166 bp) are the substrates of phage excision. In *E. coli* and in the in vitro reactions, additional DNA-bending accessory proteins are required; integration requires the host-encoded integration host factor (IHF) protein and in addition, excision requires the phage-encoded excisionase protein (Xis). The latter protein can be partially compensated for by the host-encoded factor for inversion specificity (Fis) protein (reviewed in [1,9,27]).

The wild-type *int* gene of HK022 has been introduced and shown to be active in mammalian and plant cells [7,10]. Both types of reactions (*attB* × *attP* and *attR* × *attL*) can occur without the prokaryotic accessory proteins (IHF and Xis). In the case of Int- λ , only IHF-independent mutants are active in mammalian cells [4]. The Int system can therefore serve as a potential tool for gene manipulations in the eukarya.

* Corresponding author. Tel.: +972 3 640 9823; fax: +972 3 640 6834.

E-mail address: kolott@post.tau.ac.il (M. Kolot).

Moreover, owing to its heterogeneous pairwise substrates, the Int system may operate in RMCE reactions without the need to use mutated sites.

A version of the λ Int system, known as Gateway cloning technology, has been developed by Life Technology Inc. as an in vitro gene cloning system that replaces the need for restriction and ligation in DNA cloning procedures. This system is based on an Int- λ catalyzed in vitro integrative RMCE reaction in which the gene to be cloned is flanked by two *attB* sites that are compatible with two *attP* sites on the vector. In the Gateway system all recombination reactions are carried out in vitro and the complete RMCE products are selected in *Escherichia coli* using a positive selection marker (antibiotic resistance) and a negative selection marker (*ccdB*). However, no data are available on the ability of Int to catalyze an RMCE reaction in vivo. Since our goal is to develop the Int-HK022 system for an in vivo RMCE gene replacement in the eukarya, it was essential to examine first how Int-HK022 catalyzes an RMCE in vivo in *E. coli* without a negative selection force. In the present paper, we show that the wild-type Int of phage HK022 can catalyze integrative and excisive RMCE reactions in *E. coli* as well as in vitro. An analysis of co-integrated intermediates and of protein–DNA complexes, using atomic force microscopy (AFM), suggests that the RMCE reaction may be sequential.

2. Materials and methods

2.1. Bacteria, growth conditions, plasmids and oligomers

E. coli K12 *recF* (strain DS941, [25]) served as the bacterial host. Cells were grown and plated on Luria–Bertani Rich

medium with proper antibiotics. Plasmid transformations were performed by electroporation [22]. Plasmids used in this work and oligomers used as PCR primers are listed in Table 1.

2.2. Plasmid constructions

2.2.1. pMK155

The BglIII–HindIII (*int*) fragment of plasmid pKH70 [13] was cloned between the same sites of the kanamycin-resistant (Km^R) vector pOK12.

2.2.2. pMK169

The EcoRI–HindIII (*int*–*xis*) fragment of pNK1773 [28] was cloned between the same sites of vector pOK12 [26].

2.2.3. pNA871

One *attL* site was extracted from plasmid pMK25 and inserted into the pBluescript Ap^R vector (Fermentas) between the KpnI + SalI sites. Next, a PCR fragment that carries the Tc^R gene was generated from vector pACYC184 (NEB Inc.) as template and oligomers oEY378 + oEY379 as primers and was cloned into the EcoRI site via the pGEM-T-Easy vector (Promega). The second *attL* fragment was generated by PCR from pMK25 with primers f + r and inserted between the PstI and NotI sites via vector pGEM-T-Easy.

2.2.4. pNA865

One *attR* site was extracted from plasmid pMK24 and cloned into the pBluescript vector between the KpnI and HindIII sites. A PCR fragment that carries the Cm^R gene was generated by PCR from vector pACYC184 using primers oEY376 + oEY385 and was cloned into the HindIII site. The

Table 1
List of plasmids and oligomers used as primers for PCR reactions

Plasmid name	Characteristics	Source or reference
pMK24	<i>attR</i> in pUC18, Ap ^R	[8]
pMK25	<i>attL</i> in pUC18, Ap ^R	[8]
pMK129	<i>intF</i> on pETI-1	[12]
pMK155	<i>int</i> in pOK12, Km ^R	This work
pMK169	<i>int</i> + <i>xis</i> in pOK12, Km ^R	This work
pNA865	<i>attR</i> - Cm ^R - <i>attR</i>	This work
pNA871	<i>attL</i> -Tc ^R - <i>attL</i> , Ap ^R	This work
pNA890	<i>attP</i> -Cm ^R - <i>attP</i> , Ap ^R	This work
pNA929	<i>attB</i> -Tc ^R - <i>attB</i>	This work
B. Oligomers		
Primer	Sequence (5' → 3') ^a	Location
oEY135	AGGTCACATAACTATCTAAGTAGTTGATTCATAGGACCTGG	P arm of <i>att</i>
oEY202	TAATACGACTCACTATAGGG	T7 promoter
oEY279	GGAATTAACCCTCACTAAAGGG	T3 promoter
oEY376	CCCAAGCTTCGGGAAGCCCTGGGCC	Cm ^R gene
oEY385	CCCAAGCTTCAGGCGTAGCACCAGGCG	Cm ^R gene
oEY378	GATAAGCTTTAATGCGGTAG	Tc ^R gene
oEY379	CCGAATTCACCCGTGGCCAGGACC	Tc ^R gene
oEY451	GGGAACCTTTTTCACCTAAAGTGCCACCCGTGGCCAGGACC	<i>attB</i> -Tc ^R
oEY452	GGGAACCTTTTTCACCTAAAGTGCGCACCTGAAGTCAGCCCC	<i>attB</i> -Tc ^R
Forward (f)	GCCAGGGTTTTCCAGTCACGA	Bluescript, pUC18
Reverse (r)	GAGCGGATAACAATTTTCACACAGG	Bluescript, pUC18

^a Restriction site and *attB* sequence are in boldface.

second *attR* site was extracted from pMK24 using HindIII and SacI sites, the HindIII site was blunt-ended and the resulting fragment was cloned between the SmaI and SacI sites. The *Ap^R* gene of pNA865 was partially deleted by restriction with AvaII, followed by filling in and self ligation.

2.2.5. pNA890

This plasmid was a product of the RMCE excisive reaction (Fig. 2C).

2.2.6. pNA929

The complete *attB*-Tc^R-*attB* cassette was generated by PCR using pACYC184 as template and oligomers oEY451 + oEY452 as primers. The PCR product was cloned into vector pGEM-T-Easy. The *Ap^R* gene was partially deleted by restriction with PvuI, followed by self ligation.

2.3. In vitro site-specific recombination reactions

In the integration assays, the reaction mixture (20 µl) contained 50 mM KCl, 50 mM Tris-HCl pH 7.5, 1 mM EDTA, 1 mg/ml BSA, 0.1 µM Int and 0.1 µM IHF and the appropriate plasmid substrates at a concentration of 0.6 nM. In the excision assay, 0.2 µM Xis were added. The reactions lasted for 60 min. Following heat inactivation, the reaction mixtures were used to transform *E. coli recF* cells. The reaction used for AFM imaging was not heat-inactivated; 5 mM MgCl₂ were added, whereas EDTA and BSA were omitted.

2.4. AFM imaging

Excisive circular × linear reaction products were adsorbed onto mica surfaces essentially as described [2]. Forty microliters of 0.1 nM (in molecules) DNA solution in 4 mM HEPES, pH 7.0 containing 2 mM MgCl₂ and 25 mM NaCl were deposited on freshly cleaved moskovite mica plates and incubated for 20 min, washed with distilled water and dried with nitrogen gas. AFM images were obtained with a Solver PRO (NT-MDT, Russia) AFM in non-contact (tapping) mode using Si-gold-coated cantilevers (NT-MDT) 130 µm long with resonance frequency of 119–180 kHz and a diameter of 10 nm. The images were “flattened” (each line of the image was fitted to a second-order polynomial and the polynomial was then subtracted from the image line) by the AFM’s image processing software. The contour length of individual well-separated DNA molecules was measured and averaged using Nanotec Electronica S.L. (Madrid) WSxM imaging software [11]. The length values are corrected for the finite tip radius by subtracting the molecule’s apparent width (a good approximation for the tip diameter) from the measured length.

3. Results and discussion

3.1. Integrative (*attP* × *attB*) RMCE reactions

The RMCE reactions were performed between two plasmids. In the integrative (*attP* × *attB*) reactions one plasmid

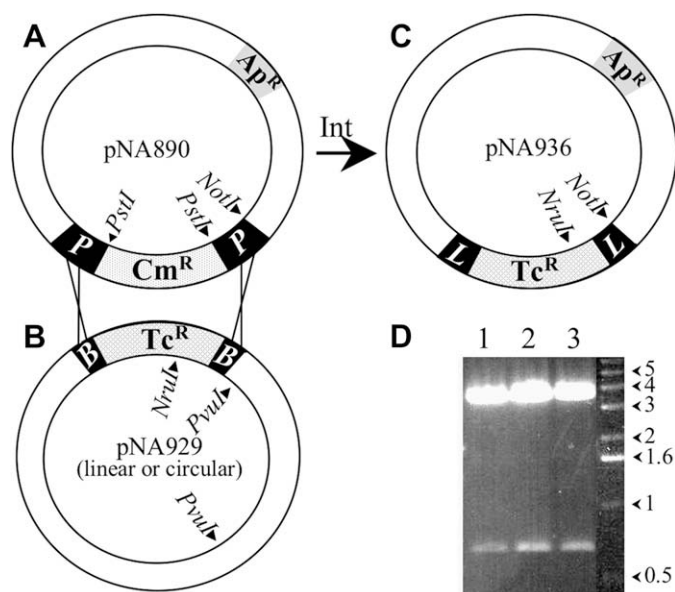


Fig. 1. A scheme of the two plasmids, pNA890 (A) and pNA929 (B), used as substrates in the integrative RMCE reaction, and the expected selectable product (C). (D) Samples of NotI + NruI RMCE products obtained in: lane 1, in vivo, two circle reaction; lane 2, in vitro, two circle reaction; lane 3, in vitro, circular × linear reaction. Right arrowheads show molecular weight markers in kb.

(pNA890, Fig. 1A) carried a chloramphenicol resistance (*Cm^R*) gene flanked by two inverted *attP* sites, as well as an ampicillin resistance (*Ap^R*) gene. The other plasmid (pNA929, Fig. 1B) carried a tetracycline-resistance (*Tc^R*) gene flanked by two inverted *attB* sites. An Int-promoted RMCE reaction is expected to exchange between the *Cm^R* and *Tc^R* genes in which one of the reaction products, that is *Ap^R* *Tc^R* (Fig. 1C), is partially selectable. This RMCE reaction was tested in vivo and in vitro.

In the in vivo integrative reaction, both circular substrates were co-transformed into an *E. coli recF* strain (strain DS941) carrying a compatible *Km^R* Int-expressing plasmid (pMK155) and plated for *Ap^R* *Tc^R* *Km^R* recombinant colonies. This selection was aimed at the RMCE products, but it also allowed growth of cells that carry both unreacted substrates. In order to detect RMCE products and to score their frequency, plasmid DNA was extracted from hundreds of pooled *Ap^R* *Tc^R* *Km^R* transformant colonies and was used to retransform the *recF* cells and plate them for *Ap^R* transformants. 100 *Ap^R* transformant colonies were picked on Tc and Cm plates to score for RMCE products. Of two independent experiments, only 4 and 3 colonies, respectively, carried the expected *Ap^R* *Tc^R* *Cm^S* RMCE phenotype (Table 2, line A). An NruI + NotI restriction analysis of plasmids extracted from the seven suspected *Ap^R* *Tc^R* *Cm^S* RMCE strains yielded the expected 4 kb + 0.73 kb fragments represented by one of them in Fig. 1D, lane 1. A sequence analysis of all of them (not shown) confirmed the expected recombinant inverted *attL* sites that flank the *Tc^R* gene (Fig. 1C). The phenotype of the majority of *Ap^R* transformants (94 and 96) was *Ap^R* *Tc^S* *Cm^R*, carrying parental *Ap^R* plasmid pNA890 originating from the primary transformants bearing both substrates. The remaining (2, 1) *Ap^R* transformant

Table 2
Number of RMCE products obtained (in bold) among tAp^R transformants in duplicate integrative (*attP* × *attB*) and excisive (*attL* × *attR*) reactions

Reaction	Substrates	Frequency of integrative products (Ap ^R Tc ^R)	Frequency of excisive products (Ap ^R Cm ^R)
A. In vivo	Circular × circular	4/100, 3/100	4/100, 6/100
B. In vitro	Circular × circular	2/100, 5/100	47/100 , 58/100
C. In vitro	Linear × circular	7/7 , 8/8	15/15 , 16/16

colonies were Ap^R Cm^R Tc^R carrying both parental plasmids either separately or as a co-integrate (see below). No RMCE products were obtained in the absence of Int.

Next, two different in vitro reactions were performed. In one, both plasmids remained circular, while in the other, one of them was linearized. In both reactions, the two DNA substrates were supplemented with purified Int and IHF and the reaction mixture was used to transform the *E. coli recF* cells that were selected for Ap^R Tc^R colonies. In the two-circles reactions, plasmid extract from many pooled Ap^R Tc^R colonies of two independent experiments was used to retransform *recF* cells followed by selection of Ap^R transformant colonies. Of 2 × 100 Ap^R colonies tested by plate picking, 2 and 5, respectively, carried the expected RMCE Ap^R, Tc^R, Cm^S phenotype (Table 2, line B). Again, the majority (95 and 90) were Ap^R Tc^S Cm^R, carrying the parental plasmid pNA890. The rest (3, 5) Ap^R transformant colonies were Ap^R Cm^R Tc^R carrying both parental plasmids either separately or as a co-integrate. Plasmid purified from each of the 7 suspected RMCE recombinant colonies (Table 2, line B) proved to carry the selected RMCE product showing the same NruI + NotI restriction pattern as above (Fig. 1D, lane 2) and their sequence revealed the recombinant *attL* sites (not shown). No RMCE products were obtained in the absence of Int.

In two independent linear × circular in vitro reactions plasmid pNA929 was linearized with PvuI prior to the reaction, whereas plasmid pNA890 remained circular. Here, the first selection for Ap^R Tc^R resulted in only 7 and 8 Ap^R Tc^R colonies (Table 2, line C), and all proved to be Cm^S, which is the expected RMCE phenotype. No colonies were obtained in the absence of Int. The NruI + NotI restriction analysis of plasmids extracted from all seven recombinant colonies yielded the same 4 kb + 0.73 kb fragments represented in Fig. 1D, lane 3. The sequence performed in 4 of the recombinant plasmids confirmed the expected recombinant inverted *attL* sites (not shown). The low yield of Ap^R Tc^R transformants in the first transformation cycle was probably due to the fact that a cross-over between a linear and a circular substrate through recombination between one pair of *att* sites results in a linear product that, upon transformation, is not able to replicate. The only RMCE product that can survive this transformation is one that has resulted from a crossover in the second pair of *att* sites that lead to a circular product.

In each of the three experiments described above, the RMCE products resulted from integrative (*attB* × *attP*) RMCE recombination, and in both circular × circular reactions they appeared at a frequency of 2–5% of the Ap^R transformants.

3.2. Excisive (*attL* × *attR*) RMCE reactions

Though the *attL* × *attR* reaction is used for phage excision, we refer to the “excisive” RMCE reactions similarly to the integrative reactions, except that the two pairs of recombining sites are *attL* × *attR*. As above, two plasmids were constructed as substrates for the in vivo and in vitro excisive reactions. One of them (pNA871, Fig. 2A) carried the Tc^R gene flanked by two inverted *attL* sites as well as the Ap^R gene. The other plasmid (pNA865, Fig. 2B) carried the Cm^R gene flanked by two inverted *attR* sites. As above, we performed one in vivo and two in vitro reactions. In the in vivo reaction, the *recF* host carrying the Int + Xis-expressing plasmid (pMK169) was co-transformed with the two circular plasmids. A pool of Ap^R Cm^R Tc^R transformants were used to retransform the *recF* host and plated for Ap^R colonies. Picking of 100 colonies from each of two independent experiments revealed 4 and 6 Ap^R Cm^R Tc^S strains of the expected RMCE phenotype (Table 2, line A). Their RMCE genotype was confirmed by NcoI + NotI restriction that showed the expected 4.8 kb and 0.95 kb fragments (Fig. 2D, lane 1), and by their sequence (not shown) that revealed the two inverted *attP* sites flanking the Cm^R gene (Fig. 2C). All the rest of the 200 Ap^R transformants showed the parental Ap^R Cm^S Tc^R phenotype of the Ap^R parent, and none showed the presence of the two parental plasmids. No RMCE phenotype was obtained in the absence of Int.

In the in vitro excisive reactions, the two substrates were supplemented with purified Int, IHF and Xis. When both substrates were circular, each of two reaction mixtures was used to transform the *E. coli recF* cells followed by the selection for Ap^R Cm^R recombinant colonies (Fig. 2C). Plasmids extracted from pooled colonies were used to retransform

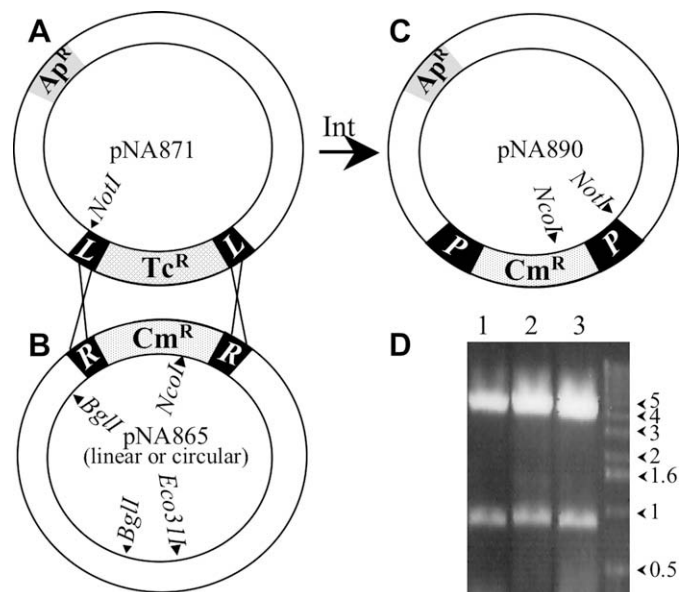


Fig. 2. A scheme of the two plasmids, pNA871 (A) and pNA865 (B), used as substrates in the excisive RMCE reaction and the expected selectable product (C). (D) Samples of NotI + NcoI RMCE products obtained in: lane 1, in vivo, two circle reaction; lane 2, in vitro, two circle reaction; lane 3, in vitro, circular × linear reaction. Right arrowheads show molecular weight markers in kb.

recF cells followed by the selection of Ap^R transformants. Surprisingly, of the 2 × 100 Ap^R transformant colonies, 47 and 58 were of the Ap^R Cm^R Tc^S RMCE phenotype (Table 2, line B). The RMCE genotype of 9 strains was confirmed as above by restriction (Fig. 2D, lane 2) and sequence analysis (not shown). Forty-eight of 100 and 40/100 of the remaining Ap^R transformants were Ap^R Tc^R Cm^S carrying the phenotype of the Ap^R parental plasmid pNA871. The remaining 5/100 and 2/100 transformants were Ap^R Cm^R Tc^R, carrying both plasmids separately or as co-integrates. No RMCE products were detected in the control experiments.

Finally, for the in vitro excisive reaction between a linear and a circular substrate, plasmid pNA865 was linearized with BglII prior to the reaction and its partner, plasmid pNA871, remained circular. As in the similar integrative reaction above, the first round of two independent Ap^R Tc^R selections yielded 15 and 16 transformants, all of which were of the RMCE Ap^R Cm^R Tc^S phenotype, as confirmed by restriction (sFig. 2D, lane 3) and sequencing (not shown) of five of them. No colonies were obtained in the absence of Int.

The results of the excisional in vivo reaction and those of the linear × circular in vitro reaction resemble the integrative reaction. The reason for the exceptionally high yield of RMCE products (~50%) that was observed between the two circular plasmids in the in vitro reaction and that repeated itself in a third experiment (not shown) is unclear. A possible explanation might be that in the excisive reaction, in contrast to the integrative one, each recombining site (*attL* and *attR*) carries an arm that can form a tight protein–DNA complex that stimulated the reaction by excess purified Int + Xis.

3.3. Analysis of co-integrate intermediates

As mentioned above, the few transformants that were resistant to all three antibiotics (Ap^R Cm^R Tc^R) could carry both substrates separately or as a single co-integrate that might have resulted from an Int-catalyzed site-specific reaction between a single pair of *att* sites (Fig. 3A–C). To test this possibility, intact plasmid extracted from the seven Ap^R Cm^R Tc^R clones obtained in the in vitro circular × circular excisional reaction was examined on a gel. The electrophoretic mobility of two was slower compared to the mobility of the other five that migrated like a monomeric control (not shown). When plasmids extracted from each of the two slower ones were linearized with NcoI (Fig. 3E, lanes 3 and 4), the size in kb of their 8.7 kb single fragment agreed with the combined lengths of their two linearized monomeric substrates (Fig. 3E, lanes 1 and 2), indicating that these two were indeed co-integrates. PCR analyses using the primers depicted by arrows in Fig. 3C has shown that the Cm^R gene was flanked on one side by the original *attR* site (Fig. 3F, primers a + b), whereas the other flanking site was the recombinant *attP* (primers b + c). Of four possible options of a single *attL* × *attR* crossover, these two co-integrates have resulted from the single *attL* × *attR* crossover that is depicted in Fig. 3A–C. Since, in these two substrates, the vector was the same (pBluescript) in two of the four possible crossover options, the sequence of the vector that flanks the recombining

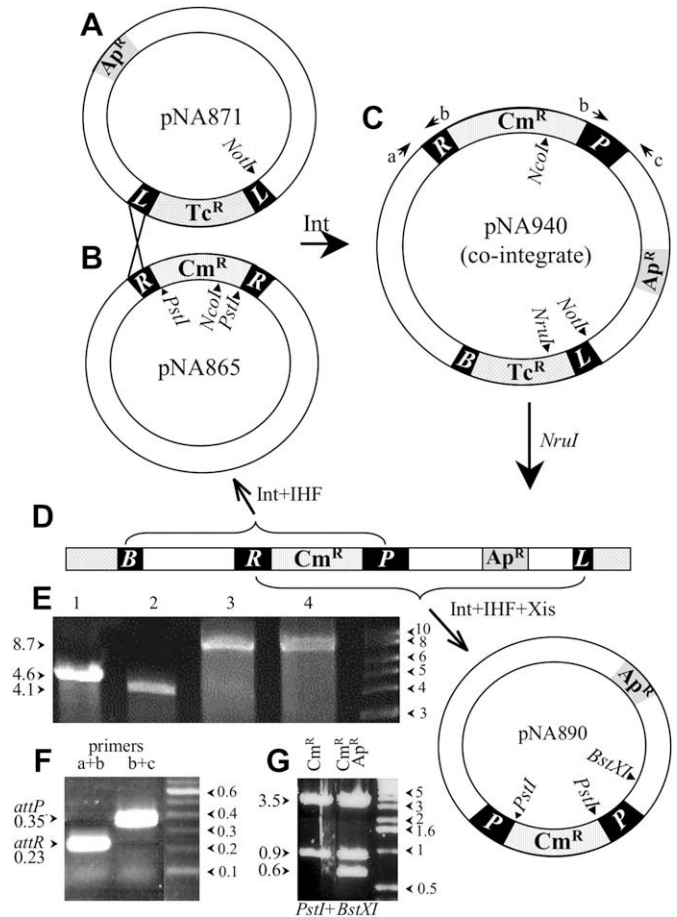


Fig. 3. (A–C) Formation of a co-integrate as a result of one site-specific crossover. The small arrows in C indicate primers used in PCRs to identify the type of *att* sites; a, oEY279; b, oEY135; c, oEY202. (D) Linear co-integrate showing the formation of the circular integrative Cm^R product (upper arrow) and the circular excisive Ap^R Cm^R product (lower arrow). (E) Gel electrophoresis of linearized plasmids: lane 1, pNA871 linearized with NotI; lane 2, pNA865 linearized with NcoI; lanes 3 and 4, two co-integrates linearized with NcoI. Left arrowheads show relevant sizes in kb, arrowheads on the right show molecular weight markers. (F) PCR product using oligomers c + b as primers and co-integrate as template (lane 1). (G) PstI + BstXI restriction pattern of Cm^R *attB* × *attP* and Cm^R Ap^R *attL* × *attR* recombinants that arose from the linear co-integrate.

cassettes is homologous, which encourages a better synapsis; these two co-integrates have resulted from one of them. Other possible co-integrates were not analyzed.

The formation of co-integrates might indicate their being intermediates in the RMCE reaction and therefore it was interesting to determine whether the RMCE reaction occurs simultaneously on both pairs of *att* sites, or whether it is a sequential reaction, namely, recombination between one pair of *att* sites leading to formation of a co-integrate is followed by recombination between the second pair of *att* sites leading to the RMCE product.

The few transformants obtained in the integrative and excisive in vitro linear × circular reactions all proved to carry RMCE products already after the first selection round (Table 2, line C). In case of a sequential reaction, a crossover between one pair of *att* sites leads to a linear substrate that is unable to

replicate. Its replication can be resumed only if a crossover in the second *att* sites follows, leading to a replicable circular RMCE product. It has been previously reported that in λ 's site-specific recombination, at least one of the substrates must be supercoiled [17], and when a supercoiled substrate is nicked, the reaction efficiency is strongly reduced [14]. These results stimulated us to test whether an integrative and/or excisive reaction on a linear substrate is possible. To do that, the circular co-integrate shown in Fig. 3C was linearized with NruI (Fig. 3D), thereby obtaining a linear product that carries all four *att* sites and two resistance markers (Ap^{R} and Cm^{R} , Fig. 3D). In order to test the ability of Int to catalyze the integrative (*attP* \times *attB*) and the excisive (*attL* \times *attR*) reactions on the linear DNA, we performed each reaction in vitro using the linearized co-integrate as substrate. For the integrative reaction, we treated the linear substrate with Int + IHF which, upon an *attP* \times *attB* reaction, is expected to form circular Ap^{S} Cm^{R} plasmids (Fig. 3D, upper arrow) that are identical to the pNA865 substrate (Fig. 3B). For the excisive reaction, the linear substrate was supplied with Int + IHF + Xis that, upon an *attL* \times *attR* reaction, is expected to form circular Ap^{R} Cm^{R} plasmids (Fig. 3D, lower arrow) that are identical to the pNA890 substrate (Fig. 1A). Each of the two reactions was used to transform *E. coli recF* cells following selection for Cm^{R} transformants. In the integrative reaction 4 Cm^{R} colonies were obtained, each, as expected, being Ap^{S} . The excisive reaction yielded 8 Cm^{R} colonies, 2 of which were Ap^{R} Cm^{R} (excisive products) and 6 were Ap^{S} Cm^{R} (integrative products). The structure of both integrative and excisive products was confirmed by PstI + BstXI restriction analysis presented for the *attB* \times *attP* Cm^{R} products in Fig. 3G, left lane, and for the *attL* \times *attR* Cm^{R} Ap^{R} products (central lane). In both reactions, no Cm^{R} transformants were obtained in the absence of Int. These results confirm that, in vitro, Int can catalyze both the integrative and the excisive reactions also on a linear substrate. Assuming that this is also possible in vivo, the formation of few but complete RMCE products that were obtained in the linear \times circular in vitro reactions can be explained by a sequential mode of the RMCE reaction, in which case linear co-integrates that underwent the second recombination reaction have resulted in an RMCE circular product that has survived the selection.

3.4. Visualization of synaptic complexes

We used AFM to visualize the products of an in vitro RMCE reaction. The products of an in vitro excisive recombination reaction between linearized and circular substrates were subjected to an AFM analysis. Plasmid pNA865 (Fig. 2B) was linearized with Eco31I while plasmid pNA871 (Fig. 2A) remained circular. In the presence of purified wild-type Int, we were not able to detect any interplasmid complexes mediated by Int probably because the wild-type enzyme had completed the reaction. In order to surmount this problem, we used IntF, a mutated Int-HK022 whose active Tyr³⁴² has been replaced by Phe (plasmid pMK129). In λ and HK022 this mutated protein is inactive and in λ its binding ability to the *att* site is unaffected

[12,20]. The mutated recombinase was mixed with IHF and Xis and incubated in the reaction buffer for 60 min. The reaction mixture was deposited on freshly cleaved mica, dried and visualized by AFM as described in Section 2. The AFM images (Fig. 4A) showed mostly single circular and linear DNA molecules as well as free protein molecules that appeared as bright spots on the image. About 5% of the DNA molecules were linked together by the proteins. A blown-up image of such a complex, seen in Fig. 4A, is shown in Fig. 4B and another one in Fig. 4C. The average contour lengths of 42 circular and 59 linear single molecules are equal to 1400 ± 25 and 1250 ± 20 nm, respectively. The length of linear fragments extruding from four complexes were equal to 393.7 ± 77.4 nm and 787.5 ± 103.1 nm. These lengths correspond nicely with the expected length of the 4.62 kb of pNA871 and 4.1 kb of pNA865 plasmids, assuming that the distance between the adjacent base pairs in the deposited double-stranded DNA is equal to 3.4 nm [21]. In all protein–DNA complexes the plasmid molecules were bound to each other only via one pair of compatible *attL* and *attR* sites; no one complex was found in which the plasmids interacted through both pairs of the sites. This observation further supports the sequential mechanism of the RMCE reaction. The Eco31I site that was used to linearize one of the substrates (pNA865, Fig. 2B) yielded approximately equal-sized arms that extend from each end of the recombination cassette 1.28 kb and 1.36 kb. This small difference did not allow us to determine whether there is a preferable pair of *att* sites for the first recombination reaction.

In conclusion, by using partial selection, we show that the wild-type Int-HK022 system can catalyze both the integrative and the excisive RMCE reactions between the two circularized substrates in vivo in its bacterial host and also in vitro, with the latter being used by the Int- λ based Gateway cloning system. While in this work we tested the wild-type Int-HK022 and its wild-type substrates for its possible use in future RMCE gene replacement in eukaryotes, in the Gateway in vitro cloning system modified *att* sites are used to control the orientation of the RMCE reaction and, as for Int, it is not clear whether the Gateway system uses the wild type or a modified Int- λ .

In all circular \times circular reactions, our first selection was incomplete, because it also allowed growth of transformants that carried both unreacted substrates, and of co-integrates. In the second transformation, we selected only for the Ap^{R} phenotype in order to score for the frequency of transformants that carried a single RMCE products. The yield in three of the Int-HK022 catalyzed circular \times circular reactions was between 2% and 6% of the tested colonies. In contrast, the in vitro circular \times circular reaction resulted in an exceptionally high yield of RMCE products of $\sim 50\%$. These frequencies are satisfactory and are easily enriched by using a negative selection force that favors the RMCE products, as already practiced in currently applied eukaryotic RMCE reactions [6].

The detection of co-integrate intermediates, the positive RMCE activity of a linear \times circular reaction and direct imaging of the reaction products lead us to suggest that the RMCE reaction can proceed via a sequential mechanism, but does not exclude the direct mechanism in which the two

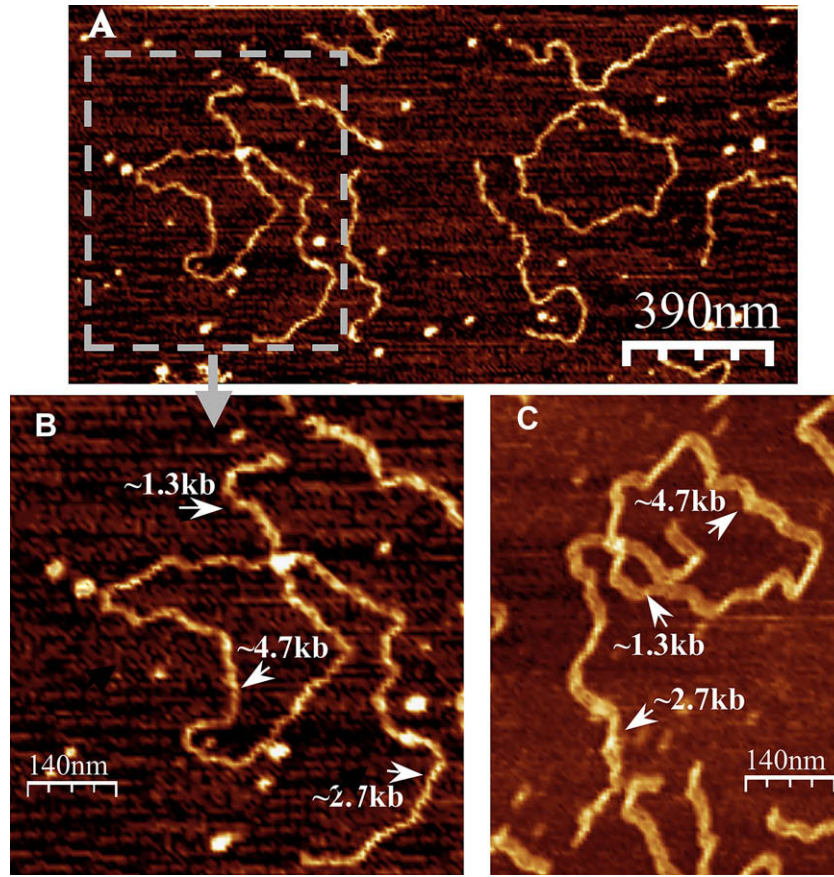


Fig. 4. (A) AFM images of the in vitro excisive reaction mix between Eco31I-linearized plasmid pNA865 and circular plasmid pNA871 showing linear substrates, a circular substrate, proteins (bright spots) and a protein–DNA complex that is blown up in B. (C) An additional protein–DNA complex. Arrows indicate sizes (in kb) of the circular substrates and two arms of the linear substrates.

crossovers occur simultaneously. Since the circular co-integrates carry two origins of replication causing their instability [24], a comparison between their frequencies and those of the complete RMCE products is problematic when drawing kinetic conclusions about the nature of the RMCE reaction.

Acknowledgments

This study was supported by a grant from the US–Israel Binational Science Foundation (grant 2003304) to E.Y. and M.K., by a grant from the Adams Supercenter for Brain Studies to M.K. and by a European grant for Future and Emerging Technologies (FP6-029192) to A.B.K.

References

- [1] Azaro, M.A., Landy, A. (2001) Integrase and the λ int family. In N.L. Craig, R. Craigie, M. Gellert, & A. Lambowitz (Eds.), *Mobile DNA II* (pp. 118–148). Washington DC: ASM Press.
- [2] Borovok, N., Molotsky, T., Ghabboun, J., Cohen, H., Porath, D., Kotlyar, A. (2007) Poly(dG)-poly(dC) DNA appears shorter than poly(dA)-poly(dT) and possibly adopts an A-related conformation on a mica surface under ambient conditions. *FEBS Lett.* 581, 5843–5846.
- [3] Branda, C.S., Dymceki, S.M. (2004) Talking about a revolution: The impact of site-specific recombinases on genetic analyses in mice. *Dev. Cell* 6, 7–28.
- [4] Christ, N., Corona, T., Dröge, P. (2002) Site-specific recombination in eukaryotic cells mediated by mutant lambda integrases: Implications for synaptic complex formation and the reactivity of episomal DNA segments. *J. Mol. Biol.* 319, 305–314.
- [5] Feng, Y.Q., Seibler, J., Alami, R., Eisen, A., Westerman, K.A., Lebouloch, P., Fiering, S., Bouhassira, E.E. (1999) Site-specific chromosomal integration in mammalian cells: highly efficient CRE recombinase-mediated cassette exchange. *J. Mol. Biol.* 292, 779–785.
- [6] Glaser, S., Anastassiadis, K., Stewart, A.F. (2005) Current issues in mouse genome engineering. *Nat. Genet.* 37, 1187–1193.
- [7] Gottfried, P., Lotan, O., Kolot, M., Maslenin, L., Bendov, R., Gorovits, R., Yesodi, V., Yagil, E., Rosner, A. (2005) Site-specific recombination in *Arabidopsis* plants promoted by Integrase protein of coliphage HK022. *Plant Molecular Biology* 57, 435–444.
- [8] Gottfried, P., Yagil, E., Kolot, M. (2000) Core-binding specificity of bacteriophage integrase. *Mol. Gen. Genet.* 263, 619–624.
- [9] Groth, A.C., Calos, M.P. (2004) Phage integrases: Biology and applications. *J. Mol. Biol.* 335, 667–678.
- [10] Harel-Levy, G., Goltzman, J., Tuby, C.N.J.H., Yagil, E., Kolot, M. (2008) Human genomic site-specific recombination catalyzed by coliphage HK022 integrase. *J. Biotechnol.* 134, 45–54.
- [11] Horcas, I., Fernandez, R., Gomez-Rodriguez, J.M., Colchero, J., Gomez-Herrero, J., Baro, A.M. (2007) A software for scanning probe microscopy and a tool for nanotechnology. *Rev. Sci. Instr.* 78, 013705.
- [12] Kolot, M., Gorovits, R., Silberstein, N., Fitchman, B., Yagil, E. (2008) Phosphorylation of the integrase protein of coliphage HK022. *Virology* 375, 383–390.
- [13] Kolot, M., Silberstein, N., Yagil, E. (1999) Site-specific recombination in mammalian cells expressing the Int recombinase of bacteriophage HK022. *Mol. Biol. Rep.* 26, 207–213.

- [14] Lange-Gustafson, B.J., Nash, H.A. (1984) Purification and properties of Int-h, a variant protein involved in site-specific recombination of bacteriophage lambda. *J. Biol. Chem.* 259, 12724–12732.
- [15] Langer, S.J., Ghafoori, A.P., Byrd, M., Leinwand, L. (2002) A genetic screen identifies novel non-compatible IoxP sites. *Nucleic Acids Res.* 30, 3067–3077.
- [16] Lauth, M., Spreafico, F., Dethleffsen, K., Meyer, M. (2002) Stable and efficient cassette exchange under non-selectable conditions by combined use of two site-specific recombinases. *Nucleic Acids Res.* 30, e115.
- [17] Mizuuchi, K., Nash, H.A. (1976) Restriction assay for integrative recombination of bacteriophage lambda DNA in vitro: requirement for closed circular DNA substrate. *Proc. Natl. Acad. Sci. U.S.A.* 73, 3524–3528.
- [18] Oumard, A., Qiao, J., Jostock, T., Li, J., Bode, J. (2006) Recommended method for chromosome exploitation: RMCE-based cassette-exchange systems in animal cell biotechnology. *Cytotechnology* 50, 93–108.
- [19] Ow, D.W. (2002) Recombinase-directed plant transformation for the post-genomic era. *Plant Mol. Biol.* 48, 183–200.
- [20] Pargellis, C.A., Nunes-Düby, S.E., de Vargas, L.M., Landy, A. (1988) Suicide recombination substrates yield covalent lambda integrase-DNA complexes and lead to identification of the active site tyrosine. *J. Biol. Chem.* 263, 7678–7685.
- [21] Saenger, W. (1984) *Principles of Nucleic Acid Structure*. New York: Springer.
- [22] Sambrook, J., Fritsch, E.F., Maniatis, T. (1989) *Molecular Cloning: A Laboratory Manual*. Cold Spring Harbor, NY: Cold Spring Harbor Laboratory.
- [23] Sorrell, D.A., Kolb, A.F. (2005) Targeted modification of mammalian genomes. *Biotechnol. Adv.* 23, 431–469.
- [24] Summers, D.K. (1991) The Kinetics of Plasmid Loss. *Trends Biotechnol.* 9, 273–278.
- [25] Summers, D.K., Sherratt, D.J. (1988) Resolution of ColE1 dimers requires a DNA sequence Implicated in the 3-dimensional organization of the *Cer* site. *EMBO J.* 7, 851–858.
- [26] Vieira, J., Messing, J. (1991) New puc-derived cloning vectors with different selectable markers and DNA-replication origins. *Gene* 100, 189–194.
- [27] Weisberg, R.A., Gottesmann, M.E., Hendrix, R.W., Little, J.W. (1999) Family values in the age of genomics: comparative analyses of temperate bacteriophage HK022. *Annu. Rev. Genet.* 33, 565–602.
- [28] Yagil, E., Dolev, S., Oberto, J., Kislev, N., Ramaiah, N., Weisberg, R.A. (1989) Determinants of site-specific recombination in the lambdaoid coliphage HK022. An evolutionary change in specificity. *J. Mol. Biol.* 207, 695–717.